Journal of Coordination Chemistry
Vol. 65, No. 4, 20 February 2012, 616–628

Taylor & Francis
Taylor & Francis Group

A V-shaped ligand bis(*N*-methylbenzimidazol-2-ylmethyl) benzylamine with its cobalt(II) complex: synthesis, crystal structure, DNA-binding properties, and antioxidant activity

HUILU WU*, JINGKUN YUAN, YING BAI, GUOLONG PAN, HUA WANG, XINGBIN SHU and GANGQIANG YU

School of Chemical and Biological Engineering, Lanzhou Jiaotong University, Lanzhou 730070, P.R. China

(*Received 8 November 2011; in final form 19 December 2011*)

A V-shaped ligand bis(*N*-methylbenzimidazol-2-ylmethyl)benzylamine (bmbb) and its cobalt complex, $[Co(bmbb)_2](pic)_2$ (pic = picrate), have been synthesized and characterized by physico-chemical and spectroscopic methods. Single-crystal X-ray revealed that the coordination sphere around Co(II) is distorted octahedral with an N_6 ligand set from two tridentate bmbb. The DNA-binding properties of bmbb and the Co(II) complex were investigated by spectrophotometric and viscosity measurements. The results suggest that bmbb and Co(II) complex both bind to DNA *via* intercalation, and the Co(II) complex binds to DNA more strongly than bmbb. The Co(II) complex also exhibited potential antioxidant properties *in vitro* studies.

Keywords: Benzimidazole; Cobalt(II) complex; Crystal structure; DNA-binding property; Antioxidant property

1. Introduction

Transition metal complexes have extensive applications in wide ranging areas [1, 2]. Interactions between transition metal complexes and DNA have been extensively studied [3]. Transition metal complexes are currently used to bind and react at specific sequences of DNA in a search for chemotherapeutics and probing DNA, and for the development of highly sensitive diagnostic agents [4–6]. Therefore, an understanding of how these small molecules bind to DNA will be useful in the design of new compounds, which can recognize specific sites or conformations of DNA [5–7].

Benzimidazole is part of the chemical structure of vitamin B_{12} which is one of the biologically relevant natural compounds [8]. Benzimidazole and its derivatives have attracted interest because of their varied biological activities namely anticancer [9], antihypertensive [10], antiviral [11], anti-inflammatory [12], vasodilator [13], and antimicrobial [14–16]. Moreover, as a typical heterocyclic ligand, large benzimidazole rings can not only provide potential supramolecular recognition sites for $\pi \cdots \pi$

*Corresponding author. Email: wuhuilu@163.com

ISSN 0095-8972 print/ISSN 1029-0389 online
http://dx.doi.org/10.1080/00958972.2012.658512

stacking interactions, but can also act as hydrogen-bond acceptors and donors to assemble multiple coordination geometries [17]. Therefore, transition metal complexes containing benzimidazole-based ligands are subject of intensive research for their rich coordination chemistry and established and potential applications [18, 19], which gives the possibility for further research, such as design of structural probes and the development of novel therapeutics.

In the framework of our research project, we mainly focused on transition metal complexes containing benzimidazole-based ligand and exploring the reaction mechanism with DNA. In preceding reports [20–24], we investigated the coordinating ability of various benzimidazole ligands and complexes. In this article, the synthesis, characterization, DNA-binding properties, and antioxidant activity of Co(II) complex with the V-shaped bmbb are presented.

2. Experimental

2.1. *Materials and methods*

All chemicals and solvents were of reagent grade and used without purification. C, H, and N elemental analyses were determined using a Carlo Erba 1106 elemental analyzer. Electrolytic conductance measurements were made with a DDS-307 type conductivity bridge using 3×10^{-3} mol L^{-1} solutions in DMF at room temperature. IR spectra were recorded from 4000 to 400 cm^{-1} with a Nicolet FT-VERTEX 70 spectrometer using KBr pellets. Electronic spectra were taken on a Lab-Tech UV Bluestar spectrophotometer. Fluorescence spectra were preformed on a LS-45 spectrofluorophotometer. The absorbance was measured with a Spectrumlab 722sp spectrophotometer at room temperature. ^{1}H-NMR spectra were recorded on a Varian VR300-MHz spectrometer with TMS as an internal standard.

The stock solution of bmbb and Co(II) complex were dissolved in DMF at 3×10^{-3} mol L^{-1}. Calf thymus DNA (CT-DNA) and ethidium bromide (EB) were purchased from Sigma. All the experiments involving interaction of the ligand and the complexes with CT-DNA were carried out in doubly distilled water buffer containing 5 mmol L^{-1} Tris and 50 mmol L^{-1} NaCl and adjusted to pH 7.2 with hydrochloric acid. A solution of CT-DNA gave a ratio of UV absorbance at 260 and 280 nm of 1.8–1.9, indicating that the CT-DNA was sufficiently free of protein [25]. The CT-DNA concentration per nucleotide was determined spectrophotometrically by employing an extinction coefficient of 6600 $(\text{mol L}^{-1})^{-1}\,\text{cm}^{-1}$ at 260 nm [26].

Synthetic route for bmbb is shown in scheme 1.

2.2. *Synthesis*

2.2.1. Synthesis of bmbb. The precursor bis(2-benzimidazol-2-ylmethyl)benzylamine (bbb) was synthesized following a slight modification of the procedure [27]. bbb (7.34 g, 20 mmol) and potassium (1.56 g, 40 mmol) were put in tetrahydrofuran (150 mL) and the solution was refluxed on a water bath for 4 h with stirring. Then, iodomethane (5.68 g, 0.04 mol) was added to this solution. With the addition of iodomethane, the

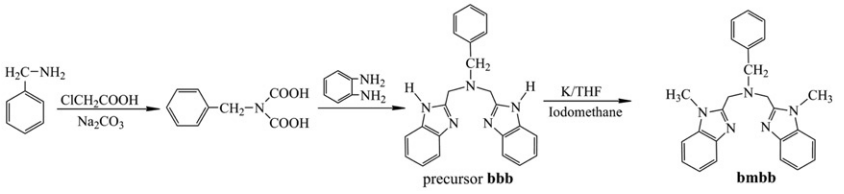

Scheme 1. Synthetic routine of bmbb.

solution gradually becomes cream yellow. The resulting solution was concentrated and cooled, a pale yellow solid separating out and the pale yellow precipitate was filtered, washed with massive water, and recrystallized from ethanol to give the ligand. Yield: 4.85 g (58%); m.p.: 185–186°C. Anal. Calcd for $C_{25}H_{25}N_5$ (%): C, 75.92; H, 6.37; N, 17.71. Found (%): C, 75.69; H, 6.54; N, 17.77. ^{1}H-NMR (DMSO-d_6 400 MHz) δ/ppm: 3.45–3.62 (s, 6H, $-CH_3$), 3.70 (m, 4H, $-CH_2$–Ar), 3.90 (m, 4H, $-CH_2$-benzimidazol), 7.23 (m, 5H, H-benzene ring), 7.27–7.61 (m, 8H, H-benzimidazole ring). UV-Vis (λ, nm): 279, 287. IR (KBr ν/cm^{-1}): 750, ν(*o*–Ar); 1230, ν(C–N); 1475, ν(C = N); 1616, ν(C = C).

2.2.2. Synthesis of [Co(bmbb)$_2$](pic)$_2$. To a stirred solution of bmbb (197.5 mg, 0.50 mmol) in hot EtOH (10 mL) was added Co(pic)$_2$ (128.78 mg, 0.25 mmol) in EtOH (2 mL). A yellow crystalline product formed rapidly. The precipitate was filtered off, washed with EtOH and absolute Et_2O, and dried under vacuum. The crude product was dissolved in MeCN to form a pale yellow solution into which Et_2O was allowed to diffuse at room temperature. Yellow crystals suitable for X-ray measurement were obtained after 2 weeks. Yield: 187.6 mg (69%). Found (%): C, 57.21; H, 4.04; N, 17.09. Calcd for $C_{62}H_{54}CoN_{16}O_{14}$ (%): C, 57.01; H, 4.17; N, 17.16. Λ_m (DMF, 297 K): 115.20 S cm^2 mol^{-1}. UV-Vis (λ, nm): 279, 281, 381, 714, 878. FT-IR (KBr ν/cm^{-1}): 746, ν (*o*–Ar); 1265, ν(C–N); 1364, ν(O–N–O); 1492, ν(C = N); 1628, ν(C = C).

2.3. *X-ray crystallography*

A suitable single crystal was mounted on a glass fiber, and the intensity data were collected on a Bruker Smart CCD diffractometer with graphite-monochromated Mo-Kα radiation ($\lambda = 0.71073$ Å) at 296 K. Data reduction and cell refinement were performed using the SMART and SAINT programs [28]. The structure was solved by direct methods and refined by full-matrix least-squares against F^2 of data using SHELXTL software [29]. All hydrogen atoms were found in difference electron maps and subsequently refined in a riding-model approximation with C–H distances ranging from 0.93 to 0.97 Å and $U_{iso}(H) = 1.2U_{eq}(C)$, $U_{iso}(H) = 1.5U_{eq}(C_{methyl})$.

2.4. *DNA-binding experiments*

2.4.1. Electronic absorption titration. Absorption titration experiments were performed with fixed concentrations of the complexes, while gradually increasing the concentration of CT-DNA. To obtain the absorption spectra, the required amount of

CT-DNA was added to both the compound and reference solutions in order to eliminate the absorbance of CT-DNA itself. From the absorption titration data, the binding constant (K_b) was determined using the equation [30]:

$$[DNA]/(\varepsilon_a - \varepsilon_f) = [DNA]/(\varepsilon_b - \varepsilon_f) + 1/K_b(\varepsilon_b - \varepsilon_f),$$

where [DNA] is the concentration of CT-DNA in base pairs, ε_a corresponds to the observed extinction coefficient (Aobsd/[M]), ϵ_f corresponds to the extinction coefficient of the free compound, ε_b is the extinction coefficient of the compound when fully bound to CT-DNA, and K_b is the intrinsic binding constant. The ratio of slope to intercept in the plot of $[DNA]/(\varepsilon_a - \varepsilon_f)$ *versus* [DNA] gave the value of K_b.

2.4.2. Fluorescence studies. The enhanced fluorescence of EB in the presence of DNA can be quenched by the addition of a second molecule [31, 32]. The extent of fluorescence quenching of EB bound to CT-DNA can be used to determine the extent of binding between the second molecule and CT-DNA. Competitive binding experiments were carried out in the buffer by keeping [DNA]/[EB] = 1 and varying the concentrations of the compounds. The fluorescence spectra of EB were measured using an excitation wavelength of 520 nm and the emission range was set between 550 and 750 nm. The spectra were analyzed according to the classical Stern–Volmer equation [33]:

$$I_0/I = 1 + K_{SV}[Q],$$

where I_0 and I are the fluorescence intensities at 599 nm in the absence and presence of the quencher, respectively, K_{sv} is the linear Stern–Volmer quenching constant, and [Q] is the concentration of the quencher. In these experiments [CT-DNA] = 2.5×10^{-3} mol L^{-1}, [EB] = 2.2×10^{-3} mol L^{-1}.

2.4.3. Viscosity titration measurements. Viscosity experiments were conducted on an Ubbelodhe viscometer, immersed in a water bath maintained at 25.0 ± 0.1°C. Titrations were performed for the complexes (3–30 μmol L^{-1}) and each compound was introduced into CT-DNA solution (42.5 μmol L^{-1}) present in the viscometer. Data were analyzed as $(\eta/\eta_0)^{1/3}$ *versus* the ratio of the concentration of the compound to CT-DNA, where η is the viscosity of CT-DNA in the presence of the compound and η_0 is the viscosity of CT-DNA alone. Viscosity values were calculated from the observed flow time of CT-DNA-containing solutions corrected from the flow time of buffer alone (t_0), $\eta = (t - t_0)$ [34].

2.5. *Antioxidant property*

Hydroxyl radicals were generated in aqueous media through the Fenton-type reaction [35, 36]. Aliquots of reaction mixture (3 mL) contained 1.0 mL of 0.10 mmol aqueous safranin, 1 mL of 1.0 mmol aqueous EDTA–Fe(II), 1 mL of 3% aqueous H_2O_2, and a series of quantitative microadditions of solutions of the test compound. A sample without the tested compound was used as the control. The reaction mixtures were incubated at 37°C for 30 min in a water bath. The absorbance was then measured

at 520 nm. All the tests were run in triplicate and are expressed as the mean and SD [37]. The scavenging effect for $OH^{\cdot}$ was calculated from the following expression:

$$\text{Scavenging ratio (\%)} = [(A_i - A_0)/(A_c - A_0)] \times 100\%,$$

where A_i = absorbance in the presence of the test compound; A_0 = absorbance of the blank in the absence of the test compound; A_c = absorbance in the absence of the test compound, EDTA-Fe(II) and H_2O_2.

3. Results and discussion

Ligand bmbb and Co(II) complex are very stable in air. The Co(II) complex is remarkably soluble in polar aprotic solvents such as DMF, DMSO, and MeCN, slightly soluble in ethanol, methanol, ethyl acetate, and chloroform, and insoluble in water, Et_2O, and petroleum ether. The molar conductivities in DMF indicate that bmbb is a nonelectrolyte while the Co(II) complex is a 1 : 2 electrolyte [38].

3.1. *IR and electronic spectra*

IR spectra of the Co(II) complex are closely related to that of free bmbb. The most diagnostic changes occur in the region between 1650 and 1250 cm^{-1}. The spectra of bmbb show a strong band at 1475 cm^{-1} and a weak band at 1616 cm^{-1}, attributed to ν(C = N) and ν(C = C) of the benzimidazole group, respectively [39–41]. These bands undergo a blue shift in the Co(II) complex as compared to free ligand, indicating participation of the imine nitrogen atoms in coordination to cobalt [42]; these are the preferred nitrogen atoms for coordination, as found in other metal complexes with benzimidazoles [43]. Moreover, information regarding bonding modes of picrate and benzimidazole rings may also be obtained from IR spectra [20].

DMF solutions of bmbb and Co(II) complex show, as expected, almost identical UV spectra. The UV bands of bmbb (287, 279 nm) are marginally red-shifted about 6 nm for the Co(II) complex, evidence of C = N coordination to the metal center. These bands are assigned to $\pi \rightarrow \pi^*$ (imidazole) transitions and the picrate bands (at 381 nm) are also assigned to $\pi \rightarrow \pi^*$ transitions [20]. The Co(II) complex exhibits two absorptions (714 and 878 nm) in visible spectra, attributed to $^4T_{1g} \rightarrow {}^4A_{2g}$, $^4T_{1g} \rightarrow {}^4T_{2g}$ transitions, respectively. This spectral pattern is typical of six-coordinate distorted octahedral cobalt. This is confirmed by the structure analysis.

3.2. *X-ray structure of the complex*

Basic crystal data, description of the diffraction experiment, and details of the structure refinement are given in table 1. Selected bond distances and angles are presented in table 2.

3.2.1. The crystal structure of $[Co(bmbb)_2](pic)_2$. The crystal structure of the Co(II) complex consists of discrete $[Co(bmbb)_2]^{2+}$ and two picrate anions. The ORTEP

Table 1. Crystal data and structure refinement for $[Co(bmbb)_2](pic)_2$.

Complex	$[Co(bmbb)](pic)_2$
Empirical formula	$C_{62}H_{54}CoN_{16}O_{14}$
Formula weight	1306.14
Temperature (K)	296(2)
Color	Brown
Crystal system	Monoclinic
Space group	*Cc*
Unit cell dimensions (Å, °)	
a	12.1784(19)
b	21.317(3)
c	23.446(4)
α	90
β	93.932(2)
γ	90
Volume (Å^3), *Z*	6072.3(16), 4
Calculated density (g cm^{-3})	1.429
F(000)	2708
Crystal size (mm^3)	$0.40 \times 0.38 \times 0.36$
θ range for data collection (°)	2.16–26.00
Limiting indices	$-15 \le h \le 15$; $-17 \le k \le 26$; $-26 \le l \le 28$
Reflections collected	16,100
Independent reflections	10,757 [$R_{int} = 0.0308$]
Refinement method	Full-matrix least-squares on F^2
Data/restraints/parameters	10,757/16/842
Goodness-of-fit on F^2	1.021
Final R_1/wR_2 indices [$I \ge 2\sigma(I)$]	0.0497/0.1008
R_1/wR_2 indices (all data)	0.0837/0.1167
Largest difference peak and hole (e Å^{-3})	0.416 and −0.348

Table 2. Selected bond distances (Å) and angles (°) in $[Co(bmbb)_2](pic)_2$.

Co(1)–N(7)	2.047(4)	Co(1)–N(5)	2.124(4)
Co(1)–N(3)	2.087(3)	Co(1)–N(1)	2.433(3)
Co(1)–N(9)	2.100(3)	Co(1)–N(6)	2.610(3)
N(7)–Co(1)–N(3)	97.33(14)	N(3)–Co(1)–N(1)	73.72(12)
N(7)–Co(1)–N(9)	107.51(14)	N(9)–Co(1)–N(1)	90.54(13)
N(3)–Co(1)–N(9)	101.45(13)	N(5)–Co(1)–N(1)	71.31(13)
N(7)–Co(1)–N(5)	97.62(14)	N(7)–Co(1)–N(6)	72.81(13)
N(3)–Co(1)–N(5)	110.59(14)	N(3)–Co(1)–N(6)	164.33(12)
N(9)–Co(1)–N(5)	136.04(14)	N(9)–Co(1)–N(6)	71.07(12)
N(7)–Co(1)–N(1)	161.31(12)	N(5)–Co(1)–N(6)	83.24(12)
N(1)–Co(1)–N(6)	119.16(11)		

structure (30% probability ellipsoids) of the $[Co(bmbb)_2]^{2+}$ with atom-numbering is shown in figure 1.

The central Co(II) is six-coordinate, by virtue of six nitrogen atoms from two tridentate bmbb. The coordination geometry of Co(II) is that of a distorted octahedron with (N1, N3, N6, and N7) providing the equatorial plane. The maximum deviation distance (N3) from the least-squares plane calculated from the four coordination atoms

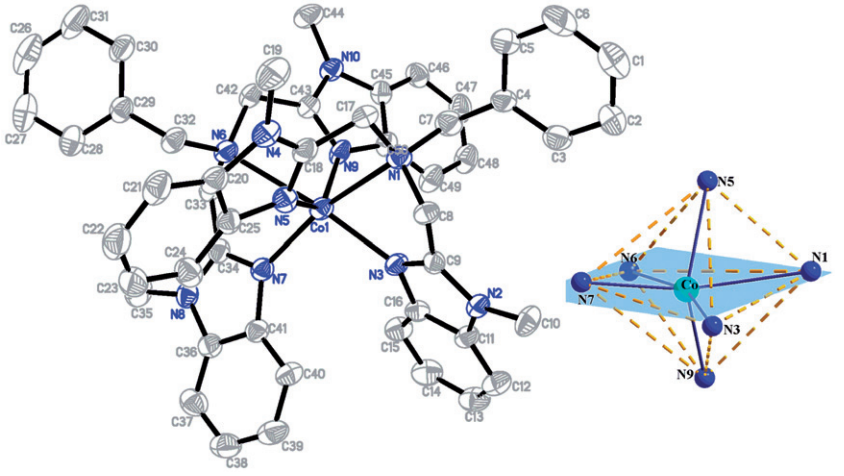

Figure 1. Molecular structure and atom-numberings of $[Co(bmbb)_2]^{2+}$ with hydrogen atoms omitted for clarity.

is 0.291 Å and Co(II) is out of this plane by only 0.013 Å. In the equatorial plane, the lengths of the bonds connected with Co(II) range from 2.047 to 2.610 Å while the bond lengths between Co(II) and the apical nitrogen atoms (N5, N9) are almost equal, average 2.112 Å. The bond angle of N5–Co–N9 in axial positions is 136.04(14)°. Therefore, compared with a regular octahedron, it reflects a relatively distorted coordination octahedron around Co(II) [44–47].

3.3. *DNA-binding properties*

3.3.1. Absorption spectroscopic studies. Electronic absorption spectra in DNA-binding studies provide bonding information. The binding of intercalative drugs to DNA has been characterized through absorption titrations, following the hypochromism and red shift associated with binding of the colored complex to the helix [30]. The electronic spectral traces of bmbb and the Co(II) complex titrated with DNA are shown in figure 2. As the DNA concentration is increased, the hypochromism reaches as high as 17.30% at 276 nm for free bmbb; 40.53% at 273 nm for Co(II) complex. The λ_{max} for Co(II) complex increases from 273 to 275 nm, slight red shifts under identical experimental conditions. The hypochromism suggests that bmbb and the Cu(II) complex interact with CT-DNA, and the spectra also imply that Co(II) complex binds to DNA more strongly than bmbb [48, 49].

To compare quantitatively the affinity of bmbb and the Co(II) complex toward DNA, the intrinsic binding constants K_b of the two compounds to CT-DNA were determined by monitoring the changes of absorbance with increasing concentration of DNA. The intrinsic binding constant K_b of bmbb and the Co(II) complex were 7.41×10^3 $(\text{mol L}^{-1})^{-1}$ ($R = 0.99$ for 16 points), 7.95×10^4 $(\text{mol L}^{-1})^{-1}$ ($R = 0.99$ for 16 points), respectively, from the decay of the absorbances. Therefore, according to

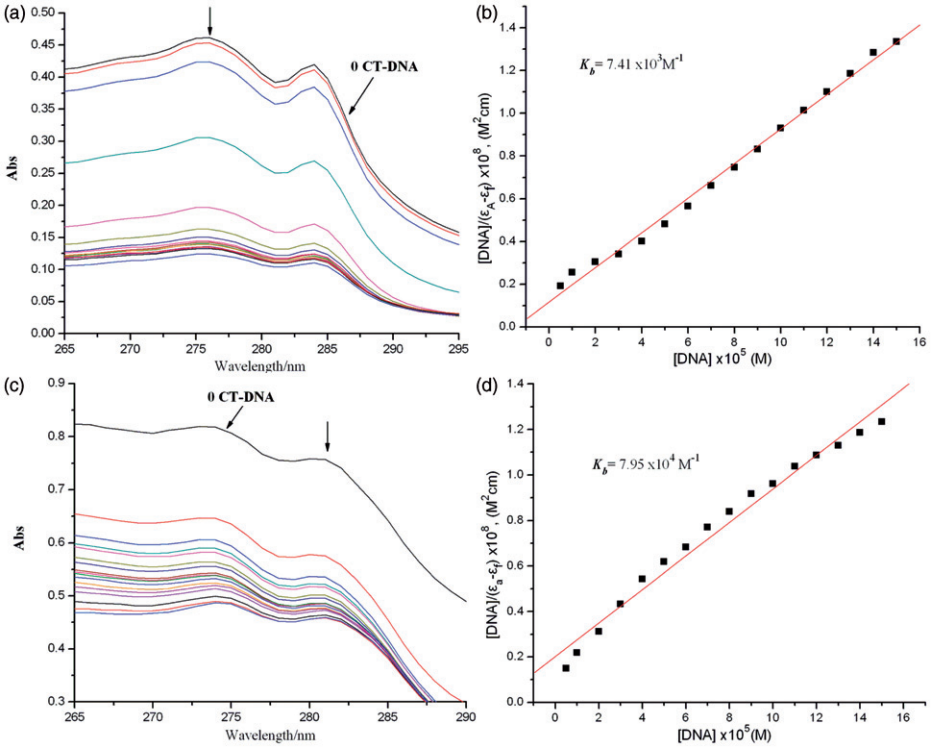

Figure 2. Electronic spectra of (a) bmbb, (c) Co(II) complex in Tris-HCl buffer upon addition of CT-DNA. [Compound] = 3×10^{-5} (mol L^{-1})$^{-1}$, [DNA] = 2.5×10^{-5} (mol L^{-1})$^{-1}$. The arrows show the emission intensity changes upon increasing DNA concentration. Plots of [DNA]/(ε_a–ε_f) *vs.* [DNA] for the titration of (b) bmbb, (d) Co(II) complex with CT-DNA.

previous reports related to DNA-intercalative cobalt complexes [50–55], we deduce that bmbb and Co(II) complex bind to DNA in an intercalation mode, due to the large coplanar aromatic rings in bmbb and Co(II) complex that facilitate it intercalating to the base pairs of double helical DNA.

Based on the above results, the affinity for DNA is stronger for Co(II) complex than ligand. We attribute three possible reasons for this difference: (i) increasing the number of planar structures may lead to higher affinity for DNA, which can be confirmed by the difference between ligand and Co(II) complex. (ii) Charge transfer of coordinated bmbb, caused by coordination of the central Co(II), results in reduction of charge density of the planar conjugated system; this change will lead to complexes binding to DNA more easily. (iii) This difference in DNA-binding ability also could be attributed to the presence of an electron deficient center in the charged Co(II) complex where additional interaction between the complex and phosphate rich DNA back bone may occur [56, 57].

3.3.2. Fluorescence spectroscopic studies. In order to further study the binding of the complex with DNA, competitive binding experiment was carried out. Relative binding of bmbb and Co(II) complex to CT-DNA was studied by the fluorescence spectral

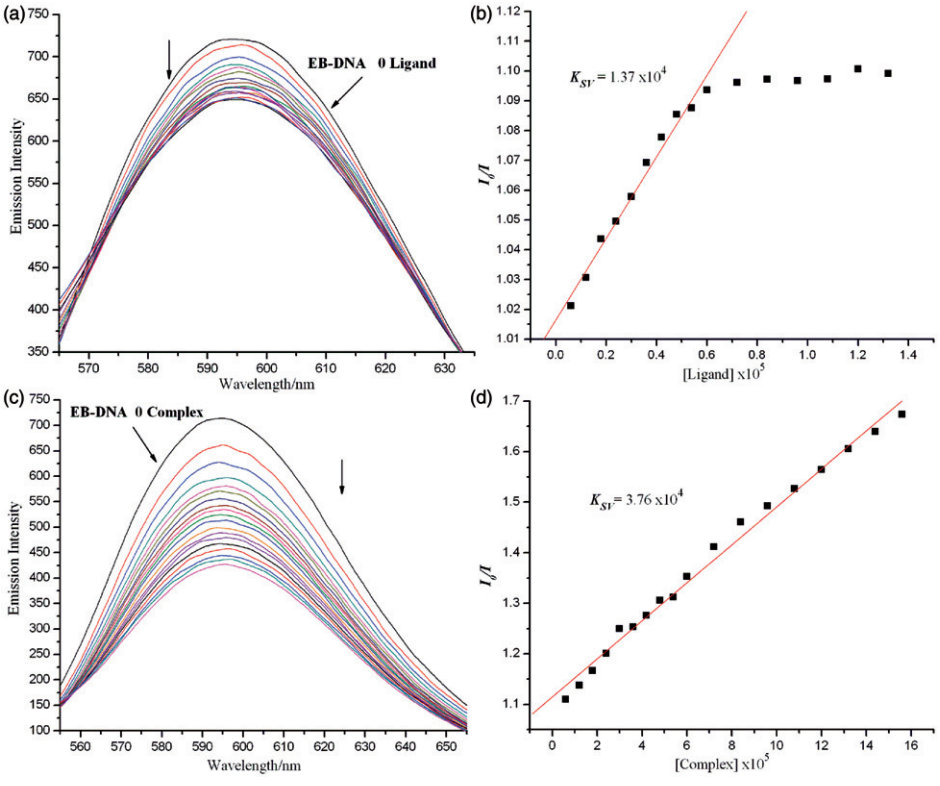

Figure 3. Emission spectra of EB bound to CT-DNA in the presence of (a) bmbb and (c) Co(II) complex; [Compound] = 3×10^{-5} mol L^{-1}; $\lambda_{ex} = 520$ nm. The arrows show the intensity changes upon increasing concentrations of the complexes. Fluorescence quenching curves of EB bound to CT-DNA by (b) bmbb and (d) Co(II) complex. (Plots of I_0/I *vs.* [Complex]).

method using EB bound CT-DNA solution in Tris-HCl/NaCl buffer (pH = 7.2). As an indicator of intercalation, EB is a weakly fluorescent compound. But in the presence of DNA, emission intensity of EB is greatly enhanced because of its strong intercalation between the adjacent DNA base pairs [32]. In general, measurement of the ability of a complex to affect the intensity of EB fluorescence in the EB-DNA adduct allows determination of the affinity of the complex for DNA, whatever the binding mode. If a complex can displace EB from DNA, the fluorescence of the solution will be reduced due to the fact that free EB are readily quenched by water [58]. For bmbb and Co(II) complex, no emission was observed either alone or in the presence of CT-DNA in the buffer. Fluorescence quenching of DNA-bound EB by the ligand and complex are shown in figure 3. The behavior of bmbb and Co(II) complex are in agreement with the Stern–Volmer equation, which provides further evidence that the compounds bind to DNA. The K_{sv} values for bmbb and Co(II) complex are 1.37×10^4 ($R = 0.99$ for 10 points in the line part) and 3.76×10^4 (mol L^{-1})$^{-1}$ ($R = 0.99$ for 16 points), respectively, reflecting the higher quenching efficiency of Co(II) complex relative to bmbb. This result suggests DNA-binding of Co(II) complex is stronger than that of bmbb, consistent with the previous absorption spectral results.

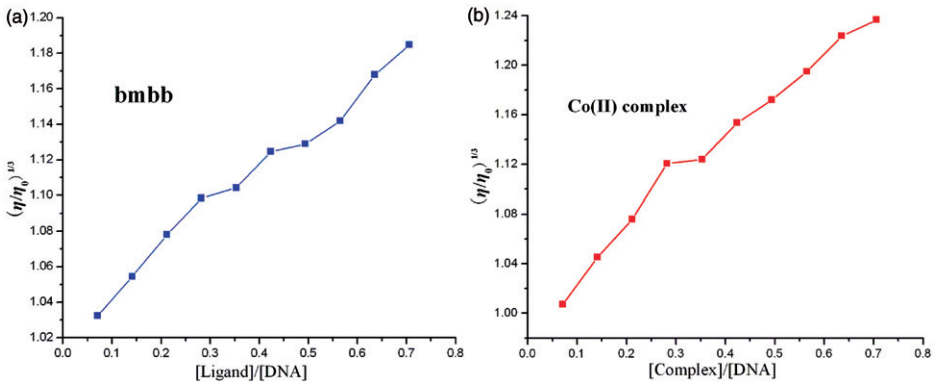

Figure 4. Effect of increasing amounts of (a) bmbb and (b) Co(II) complex on the relative viscosity of CT-DNA at 25.0 ± 0.1°C.

3.3.3. Viscosity titration measurements. Optical photophysical techniques are widely used to study the binding of ligand, metal complexes, and DNA, but do not give sufficient clues to support a binding model. Hydrodynamic measurements that are sensitive to length change (i.e., viscosity and sedimentation) are regarded as the least ambiguous and most critical tests of a binding model in solution in the absence of crystallographic structural data [25, 59]. Therefore, viscosity measurements were carried out to further clarify the interaction with DNA. In classical intercalation, the DNA helix lengthens as base pairs are separated to accommodate the bound ligand leading to increased DNA viscosity whereas a partial, nonclassical intercalation causes a bend (or kink) in DNA helix reducing its effective length and thereby its viscosity [25].

The effects of bmbb and Co(II) complex on the viscosity of CT-DNA are shown in figure 4. The viscosity of CT-DNA is increased steadily with increased amount, further illustrating that the compounds intercalate with CT-DNA. The viscosity experiments confirm intercalation into DNA base pairs already established through absorption and fluorescence spectral titration studies.

3.4. *Antioxidant property*

According to relevant reports [60–62], some transition metal complexes may exhibit antioxidant activity. We therefore also conducted an investigation to explore whether the Co(II) complex has hydroxyl radical scavenging property. We compared the abilities of our present compounds to scavenge hydroxyl radicals with those of well-known natural antioxidants mannitol and vitamin C, using the same method as reported in a previous paper [63]. The 50% inhibitory concentrations (IC_{50}) of mannitol and vitamin C are 9.6×10^{-3} and 8.7×10^{-3} $(\text{mol L}^{-1})^{-1}$, respectively. As shown in figure 5, according to the antioxidant experiments, the IC_{50} value of Co(II) complex is $7.08 \times 10^{-6}\,(\text{mol L}^{-1})^{-1}$ which implies that the Co(II) complex has the ability to scavenge hydroxyl radical. Due to the observed IC_{50} value, the Co(II) complex can be considered as a potential drug to eliminate hydroxyl radical.

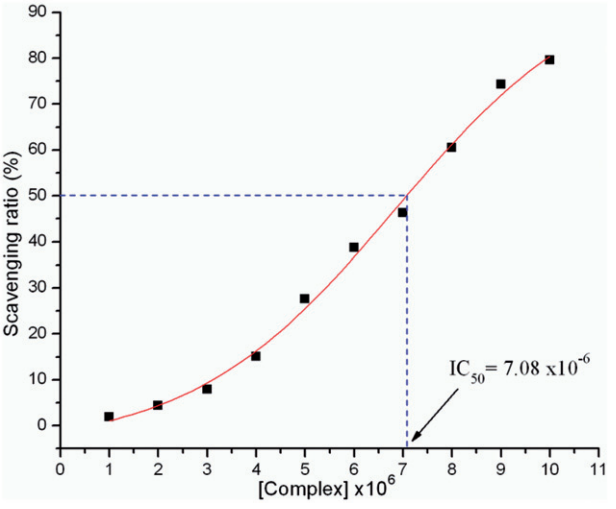

Figure 5. The inhibitory effect of Co(II) complex on OH• radicals; the suppression ratio increases with increasing concentration of the test compound.

4. Conclusion

A new ligand bis(*N*-methylbenzimidazol-2-ylmethyl)benzylamine and its Co(II) complex have been synthesized and characterized. The crystal structure of $[Co(bmbb)_2](pic)_2$ shows distorted octahedral geometry. The DNA-binding results suggest that bmbb and Co(II) complex bind to DNA in an intercalation mode, and the affinity for DNA is stronger for Co(II) complex than bmbb. The Co(II) complex can be considered as a potential drug to eliminate hydroxyl radical. These findings indicate that the Co(II) complex has practical applications for the development of nucleic acid molecular probes and new therapeutic reagents for diseases on the molecular level and warrant further *in vivo* experiments and pharmacological assays.

Supplementary material

Crystallographic data (excluding structure factors) for the structure reported in this article have been deposited with the Cambridge Crystallographic Data Centre with reference number CCDC 852827. Copies of the data can be obtained, free of charge, on application to the CCDC, 12 Union Road, Cambridge CB2 1EZ, UK. Tel: +44-01223-762910; Fax: +44-01223-336033; E-mail: deposit@ccdc.cam.ac.uk or http://www.ccdc.cam.ac.uk.

Acknowledgments

The authors acknowledge the financial support and grant from "Qing Lan" Talent Engineering Funds by Lanzhou Jiaotong University. The grant from "Long Yuan Qing Nian" of Gansu Province is also acknowledged.

References

[1] L.J.K. Boerner, J.M. Zaleski. *Curr. Opin. Chem. Biol.*, **9**, 135 (2005).
[2] C. Ahmet, T. Ülkü, C. Melek, A.K. Şengül, K. Serdar, K. Aslıgül, A.A. Faik. *Eur. J. Med. Chem.*, **45**, 5169 (2010).
[3] L.N. Ji, X.H. Zou, J.G. Liu. *Coord. Chem. Rev.*, **513**, 216 (2001).
[4] M.S. Diaz-Cruz, J. Mendieta, A. Monjonelli, R. Tauler, M. Esteban. *J. Inorg. Biochem.*, **70**, 91 (1998).
[5] K.E. Erkkila, D.T. Odom, J.K. Barton. *Chem. Rev.*, **99**, 2777 (1999).
[6] L.N. Ji, X.H. Zou, J.G. Lin. *Coord. Chem. Rev.*, **216–217**, 513 (2001).
[7] B.M. Zeglis, V.C. Pierre, J.K. Barton. *Chem. Commun.*, 4565 (2007).
[8] J.B. Wright. *Chem. Rev.*, **48**, 397 (1951).
[9] S.Y. Hong, K.W. Kwak, C.K. Ryu, S.J. Kang, K.H. Chung. *Bioorg. Med. Chem.*, **16**, 644 (2008).
[10] J.Y. Xu, Y. Zeng, Q. Ran, Z. Wei, Y. Bi, Q.H. He, Q.J. Wang, S. Hu, J. Zhang, M.Y. Tang, W.Y. Hua, X.M. Wu. *Bioorg. Med. Chem. Lett.*, **17**, 2921 (2007).
[11] P.D. Patel, M.R. Patel, N. Kaushik-Basu, T.T. Talele. *J. Chem. Inf. Model.*, **48**, 42 (2008).
[12] K. Taniguchi, S. Shigenaga, T. Ogahara, T. Fujitsu, M. Matsuo. *Chem. Pharm. Bull.*, **41**, 301 (1993).
[13] S. Estrada-Soto, R. Villalobos-Molina, F. Aguirre-Crespo, J. Vergara-Galicia, H. Oreno-DÍaz, M. Torres-Piedra, G. Navarrete-Vázquez. *Life Sci.*, **79**, 430 (2006).
[14] Ö.Ö. Guven, T. Erdogan, H. Göker, S. Yildiz. *Bioorg. Med. Chem. Lett.*, **17**, 2233 (2007).
[15] Z. Ates-Alagoz, S. Yildiz, E. Buyukbingol. *Chemotherapy*, **53**, 110 (2007).
[16] B.G. Mohamed, A.A. Abdel-Alim, M.A. Hussein. *Acta Pharm.*, **56**, 31 (2006).
[17] H.Y. Liu, H. Wu, J. Yang, Y.Y. Liu, B. Liu, Y.Y. Liu, J.F. Ma. *Cryst. Growth Des.*, **11**, 2920 (2011).
[18] J.A. Cowan. *Chem. Rev.*, **98**, 1067 (1998).
[19] C.L. Liu, M. Wang, T.L. Zhang, H.Z. Sun. *Coord. Chem. Rev.*, **248**, 147 (2004).
[20] H.L. Wu, X.C. Huang, J.K. Yuan, F. Kou, F. Jia, B. Liu, K.T. Wang. *Eur. J. Med. Chem.*, **45**, 5324 (2010).
[21] H.L. Wu, K. Li, T. Sun, F. Kou, F. Jia, J.K. Yuan, B. Liu, B.L. Qi. *Transition Met. Chem.*, **36**, 21 (2011).
[22] H.L. Wu, R.R. Yun, K.T. Wang, K. Li, X.C. Huang, T. Sun. *Z. Anorg. Allg. Chem.*, **636**, 629 (2010).
[23] H.L. Wu, X.C. Huang, J.K. Yuan, K. Li, J. Ding, R.R. Yun, W.K. Dong, X.Y. Fan. *J. Coord. Chem.*, **62**, 3446 (2009).
[24] H.L. Wu, R.R. Yun, K.T. Wang, K. Li, X.C. Huang, T. Sun, Y.Y. Wang. *J. Coord. Chem.*, **63**, 243 (2010).
[25] S. Satyanarayana, J.C. Dabrowiak, J.B. Chaires. *Biochemistry*, **32**, 2573 (1993).
[26] M.E. Reichmann, S.A. Rice, C.A. Thomas, P. Doty. *J. Am. Chem. Soc.*, **76**, 3047 (1954).
[27] K. Takahashi, Y. Nishida, S. Kida. *Polyhedron*, **3**, 113 (1984).
[28] Bruker. *SMART, SAINT and SADABS*, Bruker Axs, Inc., Madison, WI (2000).
[29] G.M. Sheldrick. *SHELXTL*, Siemens Analytical X-ray Instruments, Inc., Madison, Wisconsin, USA (1996).
[30] A.M. Pyle, J.P. Rehmann, R. Meshoyrer, C.V. Kumar, N.J. Turro, J.K. Barton. *J. Am. Chem. Soc.*, **111**, 3051 (1989).
[31] A. Wolf, G.H. Shimer, T. Meehan. *Biochemistry*, **26**, 6392 (1987).
[32] B.C. Baguley, M.L. Bret. *Biochemistry*, **23**, 937 (1984).
[33] J.R. Lakowicz, G. Webber. *Biochemistry*, **12**, 4161 (1973).
[34] C.P. Tan, J. Liu, L.M. Chen, S. Shi, L.N. Ji. *J. Inorg. Biochem.*, **102**, 1644 (2008).
[35] C.C. Winterbourn. *Biochem. J.*, **198**, 125 (1981).
[36] C.C. Winterbourn. *Biochem. J.*, **182**, 625 (1979).
[37] Z.Y. Guo, R.E. Xing, S. Liu, H.H. Yu, P.B. Wang, C.P. Li, P.C. Li. *Bioorg. Med. Chem. Lett.*, **15**, 4600 (2005).
[38] W.J. Geary. *Coord. Chem. Rev.*, **7**, 81 (1971).
[39] C.Y. Su, B.S. Kang, C.X. Du, Q.C. Yang, T.C. Mak. *Inorg. Chem.*, **39**, 4843 (2000).
[40] T.J. Lane, I. Nakagawa, J.L. Walter, A.J. Kandathil. *Inorg. Chem.*, **1**, 267 (1962).
[41] E.K. Chec, M. Kubiak, T. Glowiak, J.J. Ziolkowski. *Transition Met. Chem.*, **23**, 641 (1998).
[42] M. McKee, M. Zvagulis, C.A. Reed. *Inorg. Chem.*, **24**, 2914 (1985).
[43] K. Nakamoto (Ed.). Infrared and Raman Spectra of Inorganic and Coordination Compounds, 3rd Edn., p. 305, Wiley, New York (1978).
[44] L.E. Xiao, M. Zhang, W.H. Sun. *Polyhedron*, **29**, 142 (2010).
[45] D. Kang, J. Seo, S.Y. Lee, J.Y. Lee. *Inorg. Chem. Commun.*, **10**, 1425 (2007).
[46] N. Yoshikawa, S. Yamabe, N. Kanehisa, Y. Kai, H. Takashima, K. Tsukahara. *Eur. J. Inorg. Chem.*, 1911 (2007).
[47] J.P. Collin, I.M. Dixon, J.P. Sauvage, J.A.G. Williams, F. Barigelletti, L. Flamigni. *J. Am. Chem. Soc.*, **121**, 5009 (1999).
[48] J. Liu, T.X. Zhang, L.N. Ji. *J. Inorg. Biochem.*, **91**, 269 (2002).

[49] H. Xu, K.C. Zheng, Y. Chen, Y.Z. Li, L.J. Lin, H. Li, P.X. Zhang, L.N. Ji. *Dalton Trans*., 2260 (2003).
[50] S.A. Patil, S.N. Unki, A.D. Kulkarni, V.H. Naik, U. Kamble, P.S. Badami. *J. Coord. Chem*., **64**, 323 (2011).
[51] N. Raman, A. Selvan. *J. Coord. Chem*., **64**, 534 (2011).
[52] L.S. Kumar, H.D. Revanasiddappa. *J. Coord. Chem*., **64**, 699 (2011).
[53] N.V. Kulkarni, V.K. Revankar. *J. Coord. Chem*., **64**, 725 (2011).
[54] Q.Y. Lin, Y.Y. Wang, Y.L. Feng, D.M. Yan, Y.J. Wang, F. Zhang. *J. Coord. Chem*., **64**, 920 (2011).
[55] P. Zhao, J.W. Huang, L.N. Ji. *J. Coord. Chem*., **64**, 1977 (2011).
[56] S. Yellappa, J. Seetharamappa, L.M. Rogers, R. Chitta, R.P. Singhal, F. D'Souza. *Bioconjugate Chem*., **17**, 1418 (2006).
[57] M. Shakir, M. Azam, M.-F. Ullah, S.-M. Hadi. *J. Photochem. Photobiol. B*, **104**, 449 (2011).
[58] J.B. LePecq, C. Paoletti. *J. Mol. Biol*., **27**, 87 (1967).
[59] S. Satyanarayana, J.C. Dabrowiak, J.B. Chaires. *Biochemistry*, **31**, 9319 (1992).
[60] S.B. Bukhari, S. Memon, M. Mahroof-Tahir, M.I. Bhanger. *Spectrochim. Acta A: Mol. Biomol. Spectrosc*., **71**, 1901 (2009).
[61] F.V. Botelho, J.I. Alvarez-Leite, V.S. Lemos, A.M.C. Pimenta, H.D.R. Calado, T. Matencio, C.T. Miranda, E.C. Pereira-Maia. *J. Inorg. Biochem*., **101**, 935 (2007).
[62] Q. Wang, Z.Y. Yang, G.F. Qi, D.D. Qin. *Eur. J. Med. Chem*., **44**, 2425 (2009).
[63] T.R. Li, Z.Y. Yang, B.D. Wang, D.D. Qin. *Eur. J. Med. Chem*., **43**, 1688 (2008).